

# Resolving cell state in iPSC-derived human neural samples with multiplexed fluorescence imaging

**Martin Tomov**

Broad Institute

**Alison O'Neil**

Broad Institute

**Hamdah Abbasi**

Broad Institute

**Beth Cimini**

Broad Institute

**Anne Carpenter**

Broad Institute <https://orcid.org/0000-0003-1555-8261>

**Lee Rubin**

Department of Stem Cell and Regenerative Biology, Harvard University, Cambridge, MA 02138, USA

<https://orcid.org/0000-0002-8658-841X>

**Mark Bathe** (✉ [mark.bathe@mit.edu](mailto:mark.bathe@mit.edu))

Massachusetts Institute of Technology <https://orcid.org/0000-0002-6199-6855>

---

## Article

**Keywords:** induced pluripotent stem cell-derived (iPSC) neural cultures, PProbe-based Imaging for Sequential Multiplexing (PRISM)

**Posted Date:** January 29th, 2021

**DOI:** <https://doi.org/10.21203/rs.3.rs-152053/v1>

**License:**  This work is licensed under a Creative Commons Attribution 4.0 International License.

[Read Full License](#)

---

**Version of Record:** A version of this preprint was published at Communications Biology on June 24th, 2021. See the published version at <https://doi.org/10.1038/s42003-021-02276-x>.

1           **Resolving cell state in iPSC-derived human neural samples with**  
2                                   **multiplexed fluorescence imaging**

3  
4           Martin L. Tomov, Alison O’Neil, Hamdah S. Abbasi, Beth Cimini, Anne Carpenter, Lee  
5                                   Rubin\*, Mark Bathe\*

6                   Stanley Center for Psychiatric Research, Broad Institute of MIT and Harvard  
7                   Dept. of Stem Cell and Regenerative Biology, Harvard University  
8                   Dept. of Biological Engineering, MIT, Cambridge, MA  
9

10          Correspondence to: Lee Rubin [lee\\_rubin@harvard.edu](mailto:lee_rubin@harvard.edu) and Mark Bathe [mark.bathe@mit.edu](mailto:mark.bathe@mit.edu)

11  
12          **ABSTRACT**

13          Human induced pluripotent stem cell-derived (iPSC) neural cultures offer clinically relevant models  
14          of human diseases, including Amyotrophic Lateral Sclerosis, Alzheimer’s, and Autism Spectrum  
15          Disorder. In situ characterization of the spatial-temporal evolution of cell state in 2D and 3D culture  
16          models and organoids based on protein expression levels and localizations is essential to  
17          understanding neural cell differentiation, disease state phenotypes, and sample-to-sample  
18          variability. Here we apply Probe-based Imaging for Sequential Multiplexing (PRISM) to facilitate  
19          multiplexed imaging with facile, rapid exchange of imaging probes to analyze iPSC-derived cortical  
20          and motor neuron cultures that are relevant to psychiatric and neurodegenerative disease models,  
21          using over ten protein targets. Our approach permits analysis of cell differentiation, cell  
22          composition, and functional marker expression in both standard 2D cultures and 3D spheroid and  
23          organoid sections. Further, our approach is amenable to automation, offering in principle ability to  
24          scale-up to dozens of protein targets and samples.

## 25 Introduction

26 Induced pluripotent stem cell (iPSC)-derived cultures are increasingly becoming the principal  
27 source of patient-specific and disease-specific cellular material for *in vitro* disease modeling. iPSC-  
28 derived cortical and motor neuron cultures have successfully been used to model  
29 neurodevelopmental conditions including autism spectrum disorder (ASD; cortical neurons) [1-5]  
30 and neurodegenerative conditions including spinal muscular atrophy and amyotrophic lateral  
31 sclerosis (SMA, ALS; motor neurons) [6-9]. Such iPSC-based models are attractive because they  
32 can generate the large numbers of neural cells needed for drug screening. They can also  
33 recapitulate aspects of cortical and motor neuronal synaptic networks, which allow for functional  
34 models of neurodevelopmental and neurodegenerative conditions to be developed *in vitro*.  
35 However, phenotypic characterization of these cultures is challenging due to their complexity,  
36 heterogeneity, and variability; this provides a clear opportunity for improved high content analysis  
37 techniques, especially those that can produce multidimensional readouts from the same culture.

38 Fluorescence-based antibody staining of target markers is one approach to characterizing in situ  
39 stem-cell derived neural cultures, but is limited by the conventional spectral limit of fluorophores  
40 to imaging four targets simultaneously. One technique to overcome this limitation uses DNA-  
41 conjugated antibodies to fluorescently image more than 10 individual markers in the same sample  
42 [10, 11]. This procedure, called PRobe-based Imaging for Sequential Multiplexing (PRISM),  
43 eliminates the need for antibody stripping or removal for multiplexing, a limiting factor in traditional  
44 immunofluorescence/immunocytochemistry (IF/ICC)-based multiplexed imaging strategies [12,  
45 13], thereby allowing characterization using a greater number of molecular targets. Briefly, PRISM  
46 antibodies use short, orthogonal oligonucleotide sequences that are complementary to either a  
47 fluorophore-conjugated locked nucleic acid (LNA) or DNA strand that reversibly hybridizes to  
48 produce a fluorescent readout, analogous to traditional IF/ICC imaging [11, 14, 15] and DNA-  
49 PAINT/EXCHANGE-PAINT [14]. Further, compared to standard antibody stripping procedures  
50 [16-18], PRISM offers non-destructive imaging probe exchange, cycling fluorescent imaging  
51 strands within several minutes permitting multiple rounds of imaging data acquisition [19-21] from  
52 the same culture. These features allow the use of large panels of markers, consequently providing  
53 higher content datasets. Generation of oligo pairs is relatively straightforward due to the use of  
54 commercially available thiolated and fluorescently labelled oligo strands that can be readily  
55 conjugated to a wide variety of commercially available antibodies [11, 14, 15].

56 Here, we apply PRISM to 2D and 3D stem cell-derived cortical and motor neuron cultures to  
57 characterize cell identity and population composition based on detection of structural, synaptic,  
58 and transcription factor markers (**Figure 1**). Identification of multiple cell states within the same  
59 iPSC-derived 2D or 3D sample helps spatially map the temporal evolution and heterogeneity of  
60 targets in human samples, in addition to characterizing structural and synaptic features pertinent  
61 to human disease phenotypes [22-24]. We also introduce a CellProfiler/FIJI computational pipeline  
62 to analyze imaging data regarding cell state/phenotype in an automated, quantitative, unbiased  
63 manner [23, 24]. 2D cultures can be used for high-throughput characterization of stem cell-derived  
64 neurons, which lends itself well to automation assays, whereas 3D organoid sections retain the  
65 higher order structure of cellular organization, especially in neural cultures, which can be critical  
66 for disease modeling *in vitro*. Because PRISM is a direct analog to IF/ICC imaging, our approach  
67 complements assays in model culture systems currently used to evaluate stem cell differentiation,  
68 compound and drug candidate screening, tissue engineering, and potentially *in vitro* disease  
69 diagnostics development.

## 70 RESULTS

71 We built 12 antibodies into a PRISM panel to characterize the cellular composition of iPSC-derived  
72 CN and MN cultures. Specificity of target imaging was confirmed using traditional IF and compared  
73 to respective PRISM markers. We used established stem cell-derived astrocyte, CN, and MN  
74 cultures to screen a large panel of neural markers (**SI Table 1**)- before narrowing down to a panel  
75 of 12 PRISM-compatible antibodies (**SI Table 2, Figure 2a**). Based on staining intensity, signal  
76 specificity, and co-localizations between target markers, we were able to use 3+ specific markers  
77 to define a cell's identity (**SI Table 2 and Figure 2a**). For each selected antibody, we further  
78 compared the staining signal between IF/ICC and PRISM before and after PRISM conjugation  
79 (**Figure 2b and SI Figure 4**) to ensure each was still highly selective for its target and that the  
80 fluorescence pattern was consistent and unchanged between IF/ICC control and PRISM signal  
81 (**SI Figure 7**).

82 Newly generated DNA imaging strands were supplemented with published LNA imaging strands  
83 [11] for an initial round of 10 DNA-PRISM pairs (**SI Table 7 and SI Figure 4 and SI Figure 5**).  
84 Fluorescence signals were suitable for both manual and automated quantification of all 10 PRISM  
85 markers and 2 control IF/ICC markers (**SI Figure 6**). In order to confirm that PRISM signal is  
86 significantly above background, and thus suitable to imaging, we compared DNA-PRISM with  
87 traditional IF using cross-correlation analysis to map specific PRISM signals to subsequent IF  
88 signals in the same culture validated all 12 markers in human iPSC-derived CN (**SI Figure 7**) and  
89 in rat hippocampal neurons validated the tested markers (**SI Figure 8**). A full DNA-PRISM marker  
90 panel in rat hippocampal neurons was performed, showing that DNA-PRISM can be used to  
91 characterize neural cultures from different organisms while maintaining specificity of marker  
92 staining patterns (**SI Figure 9**).

93 Validation and optimization included matching staining patterns in primary rat hippocampal  
94 neurons and human stem cell-derived (BJ-SiPs) CN between control IF/ICC and PRISM by  
95 Pearson Correlation analysis with values ranging between 0.65 (synaptic markers) and 0.89  
96 (cytoskeletal markers), and signal-to-noise ratios of at least 25:1 based on pixel intensity [A.U.],  
97 and minimal off-target binding and non-specific signal between the validated oligos and any  
98 present cell DNA or RNA transcripts, which is necessary for imaging nuclear transcription factors  
99 and to reduce non-specific binding to native DNA and/or RNA even after salmon sperm DNA  
100 blocking and RNase treatment.

101 **PRISM enables high content imaging of over ten neural markers in 2D and 3D iPSC-derived**  
102 **CN and MN cultures.** 3D iPSC-derived CN and MN cultures were dissociated, plated in standard  
103 2D culture wells, maintained for 14 days, and then fixed and stained for analysis. First, BJ-SiPs  
104 iPSCs were differentiated into CN (**SI Table 4**) and characterized via multiple markers by  
105 traditional IF/ICC to confirm their cortical nature (**SI Figure 1**). Representative images of the 2D  
106 CN culture illustrate multiple cell subtypes (**Figure 3a**). We further characterized in-depth two time  
107 points during differentiation of cortical cultures in relation to cell identity (**Figure 3b**). At day 55 of  
108 cortical differentiation, there were 84 cells that fulfilled our analysis criteria (**Figure 2a**) where we  
109 were able to positively identify 30% of the analyzed cells as neurons. Synaptic marker staining  
110 characterized 100% of identified neurons as excitatory in this earlier culture (VGLUT1+).  
111 Immature/inactive astrocytes (CD44+/Vimentin+) made up 18% of the culture and 7% of the cells  
112 expressed markers for mature/activated astrocytes (CD44+/GFAP+). We were also able to  
113 positively identify both neural progenitor cells (2%, Pax6+) and a significant percentage of radial  
114 glial cells (36%, Pax6+/Vimentin+). Cells that were present but could not be positively identified

115 represented 7% of the total population. We then followed up with a day 85 differentiation timepoint,  
116 where we identified 161 cells that fulfilled the criteria for analysis as outlined in the Methods  
117 section. Of these, 58% were positively identified as neurons (Tuj1+/MAP2+) and 26% as  
118 astrocytes (CD44+/Vimentin+/GFAP+). Neurons were successfully further sub-typed based on  
119 synaptic marker expression into either excitatory (52%, VGLUT1+) or inhibitory (3%, VGAT+). The  
120 remaining 45% of identified neurons were not strongly associated with either type. Astrocytes were  
121 further characterized as either immature/inactive (19%, Pax6-/Vimentin+/CD44-) or mature/active  
122 (7%, Pax6-/GFAP+/CD44+). We observed no significant presence of either neural progenitor  
123 (Pax6+) or radial glial cells (Pax6+/Vimentin+). We were unable to classify 16% of cells present,  
124 based on our characterization criteria.

125 A parallel PRISM assay of iPSC-derived 2D MN cultures validated the full panel of conjugated  
126 antibodies (**Figure 4**) to characterize the MN cultures in a similar manner. To validate that the  
127 generated neuronal cells are indeed motor neurons, we stained separate wells on the same plate  
128 with the motor neurons markers Islet 1 and 200kD neurofilament protein (**SI Figure 2**)  
129 Subsequently, PRISM antibodies generated highly specific signals, and the images were then  
130 overlaid to generate high-content imaging datasets. We show here that DNA-PRISM antibodies  
131 can characterize complex stem cell-derived cultures in a multi-dimensional manner with the added  
132 ability to preserve the spatial relationships between the markers used in our characterization  
133 pipeline. Further optimization to improve staining quality by testing antibodies that are generated  
134 to produce high specificity and optimized signal-to-noise ratios in the putative MN cultures in  
135 particular is ongoing.

136 **Automated pipeline to pair PRISM high-content data analysis with high throughput data**  
137 **generation.** Due to the high volume of raw data that is generated in a PRISM imaging assay, we  
138 endeavored to develop an automated platform that could manage staining, imaging, and data  
139 analysis in the same pipeline. We first identified key points in our manual PRISM assay data  
140 acquisition process, namely buffer exchanges, imager strand incubation, and IF/ICC imaging, and  
141 automated them using a BRAVO liquid handler and a PerkinElmer Phenix spinning disk confocal  
142 microscope. Next, points of adaptation within the physical assay steps such as buffer volume,  
143 aspiration and dispensing speed, and incubation times were streamlined to improve automation.  
144 Slowing buffer aspiration and addition into the wells significantly reduced cell detachment and  
145 damage during the twenty consecutive buffer exchanges that were necessary for a complete  
146 PRISM assay. Representative PRISM staining performed with automation (**SI Figure 10a**) was  
147 comparable to manual PRISM staining and imaging (**Figure 3a**). While the average time for data  
148 acquisition was similar between the manual and automated assays, incorporating automated  
149 CellProfiler and FIJI analysis pipelines (available upon request) reduced the analysis time by  
150 almost 3-fold resulting in an overall reduction of assay duration, while increasing throughput (**SI**  
151 **Figure 10b**).

152

153 **DISCUSSION**

154 Recently, high content analysis has been used to characterize multiple neurological cell types and  
155 their interactions *in vivo* and *in vitro* [25, 26], providing insights into cell differentiation and  
156 neurological conditions [27-31]. Such work can benefit from a complementary IF method that is  
157 not constrained by limitations inherent in traditional antibody-based imaging. In our analysis, we  
158 used DNA- and LNA-conjugated PRISM antibodies to evaluate complex CN and MN cultures  
159 derived from stem cell lines in both 2D cultures and in 3D organoid sections (data not shown). In  
160 future studies, we envision that PRISM may be used for large scale analysis of neural disease  
161 initiation and progression, such as in ALS, focusing on morphology, synaptic make-up and  
162 interactions between neurons and glial cells that are present in these cultures [32].

163 We used PRISM to perform multi-dimensional characterization of heterogeneous cell types that  
164 have direct pharmacological and disease modeling applications. DNA/DNA or DNA/LNA pair  
165 strands with a number of fluorophore modifications are readily available from commercial vendors,  
166 making such antibody panels relatively straightforward to generate for a wide range of research  
167 applications. Wang et al. [33] reported that DNA-only oligos can have significant non-specific  
168 binding to native transcripts. To mitigate this issue, we implemented a salmon sperm DNA blocking  
169 step, as well as RNase pre-treatment of the fixed cultures when LNA strands were used (see **SI**  
170 **Table 3** for detailed protocol). We further chose DNA oligo pairs between 11-12 nucleotides with  
171 GC content between 30-40%, which we found to be optimal for reducing background fluorescence  
172 while still allowing complete washout or exchange of imaging strands post-acquisition. High  
173 melting temperature of the DNA/LNA oligos may push PRISM into a range where samples need  
174 to be heated, even under low salt concentration, in order to release imaging strands. High melting  
175 temperature also can cause fluorescence artifacts such as residual signal and non-specific binding  
176 and increased cell detachment due to the need for heating and cooling of the sample, thereby  
177 complicating assay automation [21, 34, 35]. While fluorescence from the PRISM staining was  
178 considerably lower than the corresponding signal from conventional secondary antibodies (**SI**  
179 **Figure 4c**), it was still well above background levels and this potential limitation could be overcome  
180 with further development of the technique to increase number of fluorophores on the imager  
181 strands, or with longer exposure times.

182 The 12 markers that we used in our assay allowed in depth analysis suggesting that disease-  
183 specific morphological and gene expression differences could be elucidated. These findings open  
184 the door to using PRISM antibodies for drug screening and characterizing *in vitro* disease models.  
185 We further expanded our fluorophore detection lines from one [11] to two, halving the time  
186 necessary for imaging and reducing the number of wash steps, which decreased cell detachment,  
187 thus improving our multi-dimensional analysis reproducibility. To take full advantage of the multi-  
188 dimensional data set that was generated, we incorporated in-depth analysis capabilities using a  
189 custom CellProfiler pipeline. This pipeline can characterize cell subsets within cultures in general,  
190 and in the cortical cultures, characterize the localization and density of synaptic markers within  
191 defined neurites. PRISM would likely be especially well suited to support studies of polygenic  
192 psychiatric conditions (Autism Spectrum Disorder and Schizophrenia), neurodevelopmental  
193 (ALS), and neurodegenerative (Parkinson's and Alzheimer's) conditions, which are characterized  
194 by multiple contributing genes and protein targets [36-42].

196 **MATERIALS AND METHODS**

197 *Consent for use of human material.* All human material (iPSC lines) was obtained with informed  
198 consent and used with the approval of the Harvard University IRB and ESCRO committees. The  
199 BJ-SiPs cell line was derived from a healthy male donor using Sendai virus reprogramming. The  
200 39B stem cell line was derived from a female donor that was positive for Amyotrophic lateral  
201 sclerosis (SOD1A4V), using retroviral integration of the transgenes Oct4, Sox2, KLF4. The 1016A  
202 stem cell line was derived from a healthy male donor using Sendai virus reprogramming.

203 *DNA-PRISM antibody marker selection, conjugation, and validation.* Starting from a list of  
204 commonly used neural culture-specific antibodies (**SI Table 1**), we chose a set of twelve markers  
205 to build the PRISM antibody panel (**Figure 2**). The antibody panel features housekeeping and  
206 structural targets ( $\alpha$ -Tubulin, Actin), markers for canonical neural culture characterization (Tuj1,  
207 Map2, Synapsin I, GFAP, Vimentin, CD44), as well as cell-specific markers, including those for  
208 identifying cortical (VGAT, VGLUT1) and motor neurons (Islet1), glial cell subtypes (Vimentin,  
209 GFAP, CD44), neural progenitor cells (Pax6), and residual pluripotent cells (Oct4A) that might  
210 have been retained post-differentiation (**SI Table 2**). For each antibody, validation was first  
211 performed using standard IF/ICC prior to oligo conjugation.

212 *Confocal imaging of control markers and PRISM panel.* Cultures were fixed in 4%  
213 paraformaldehyde for 15 min at room temperature, then washed in phosphate buffered saline  
214 (PBS) and stored at 4°C until they were stained and imaged. Immediately prior to staining, fixed  
215 cultures were quenched in 100 mM glycine in ddH<sub>2</sub>O for 10 min at room temperature. After  
216 quenching, the fixed cells were permeabilized in 0.2% Triton X-100 in PBS for 15 min at room  
217 temperature and blocked in 2% bovine serum albumin (BSA) in PBS supplemented with 1 mg/ml  
218 salmon sperm DNA (catalog #D7656; Sigma-Aldrich) for 1 hour at 4°C. For marker validation and  
219 optimization of staining conditions, cultures were imaged on a Nikon Ti-E spinning disk confocal  
220 microscope. High-content imaging with the validated conjugated antibodies panel was then carried  
221 out on a PerkinElmer Opera Phenix high-content confocal microscope. The PRISM imaging  
222 sequence was performed as previously described [11], with the following modifications. We used  
223 all primary antibodies in the panel, both in regular IF/ICC and for PRISM assays, at 1:400 dilution  
224 and all secondary fluorophore-conjugated antibodies at 1:1000 dilution for IF. Secondary PRISM-  
225 conjugated antibodies were used at 1:200 dilution. We used highly cross-adsorbed secondary  
226 antibodies raised in donkey for PRISM, to minimize any possible signal cross-talk and fluorophore  
227 conjugated secondary antibodies also raised in donkey as negative/positive controls. The full list  
228 of antibodies is provided in **SI Table 1**, with specific staining protocols for DNA-PRISM, including  
229 imaging/other buffers, provided in **SI Table 3**.

230 *Induced pluripotent stem cells (iPSCs) maintenance.* Human iPSCs (BJ-SiPs, 1016A, and 39B)  
231 were maintained feeder-free on Matrigel hESC-Qualified Matrix (catalog #354277; Corning)  
232 coated plates in StemFlex (catalog #A3349401; ThermoFisher) or mTeSR1 (catalog #85857;  
233 STEMCELL Technologies) medium to maintain pluripotency and for expansion. Both media were  
234 supplemented with pen/strep (1x; catalog #15140122; Gibco). Media were changed every other  
235 day for StemFlex and every day for mTeSR1, with cells passaged when they reached >80%  
236 confluence.

237 *Neural progenitor cells (NPCs) maintenance.* Human NPCs were generated using the STEMdiff  
238 SMADi neural induction kit (catalog #08581; STEMCELL Technologies) according to the

239 manufacturer's instructions. Briefly, dissociated iPSCs were seeded as a monolayer on Matrigel-  
240 coated plates in the provided neural induction medium (NIM) for 14 days, with daily medium  
241 changes. NPC expansion, where needed, was performed in Neural Progenitor Medium (catalog  
242 #05833; STEMCELL Technologies) from the same kit. On average, NPCs doubled every 3-5 days.

243 *Rat primary hippocampal neurons maintenance.* Dissociated rat hippocampal neurons were  
244 plated on Matrigel-coated plates and maintained in Neurobasal (NB) Medium (catalog # 21103049  
245 ThermoFisher) supplemented with B27 with insulin (1x; catalog #17504044 Gibco), non-essential  
246 amino acids (1x catalog #11140050 Gibco) and 1x pen/strep for 21 days, with half medium  
247 changes every 5 days.

248 *Human iPSC-derived cortical neuron differentiation and maintenance.* Human cortical neurons  
249 (CN) were differentiated as spheroids in a 3D spinner flask based on previously established  
250 protocols [43, 44] with some modifications. Pluripotent iPSCs were dissociated into single cell  
251 suspensions using Accutase (1x; catalog #07920 STEMCELL Technologies) for 10 minutes at  
252 37°C. Cells were then adapted to a spinner flask at a concentration of  $1 \times 10^6$  cells/mL in mTeSR1  
253 medium supplemented with rho kinase (ROCK) inhibitor, Y-27632 (10  $\mu$ M; catalog #SCM075 EMD  
254 Millipore) for 2 days. Neural progenitor patterning with the small molecules SB431542 (10  $\mu$ M;  
255 catalog #1614 Tocris), LDN193189 (1  $\mu$ M; catalog #6053 Tocris) and XAV939 (2  $\mu$ M; catalog  
256 #3748 Tocris) was carried out over the next 4 days, with full medium changes every day. Cells  
257 were grown in mTeSR1 supplemented with the above factors for the initial 24 hours, then the cells  
258 were maintained in Knockout Serum Replacement (15% KSR; Thermo Fisher Scientific) medium  
259 for the next 3 days, again supplemented with the above factors. Between days 5 to 11, we  
260 gradually transitioned the cells into NIM as follows. On day 5, 75% KSR Pulse medium was mixed  
261 with 25% NIM medium supplemented with SB431542 (10  $\mu$ M) and LDN193189 (1  $\mu$ M) and cells  
262 were incubated for 2 days. On day 7, 50% KSR medium and 50% NIM medium were  
263 supplemented with LDN193189 (1  $\mu$ M) for another 2 days. On day 9, cells were kept in 25% KSR  
264 mixed with 75% NIM medium with LDN193189 (1  $\mu$ M) for another 2 days. On day 11, the 3D  
265 cultures were fully transitioned to NIM medium for 9 days with full medium changes every 3 days.  
266 The NIM medium at this point was not supplemented with any additional small molecules. On day  
267 20, spheroids were transitioned to NB medium, supplemented with B27 Supplement (1x; catalog  
268 #A3582801 ThermoFisher), N2 Supplement (1x; catalog #17502048 ThermoFisher), brain-  
269 derived neurotrophic factor (BDNF; 10 ng/mL; catalog #248-BD-010 Tocris) and glial cell-derived  
270 neurotrophic factor (GDNF; 10 ng/mL; catalog #212-GD-010 Tocris) and maintained with full  
271 medium changes every 4 days until day 40. At this point, mitotically active cortical progenitors  
272 could be cryo-stored or maintained as spheroids for a further 14 days or more (up to 100 days) to  
273 generate mature CN for functional analysis, with 50% medium changes every 3 days. For staining  
274 and analysis, spheroids were dissociated in 0.25% Trypsin-EDTA (catalog #15575020  
275 ThermoFisher) to single cells. The cell suspension was plated into 96-well plates that were  
276 previously coated with poly-D-lysine (25  $\mu$ g/mL) and poly-L-ornithine (25  $\mu$ g/mL) overnight at 37°C,  
277 and then further coated with Laminin ((10  $\mu$ g/mL; catalog #11243217001 Sigma-Aldrich) for 3  
278 hours at 37°C. These 2D cultures were then matured for an additional 14 days prior to DNA-  
279 PRISM marker analysis, with 50% medium changes every 3 days. See **SI Table 4** for detailed  
280 protocol steps and **SI Figure 1** for representative images of cortical cultures

281 *Human iPSC-derived motor neuron differentiation and maintenance.* Motor neurons (MN) were  
282 generated using a modified version of previously established protocols [45, 46]. iPSC colonies  
283 were dissociated into single cells using Accutase. Cells were then seeded into ultra-low

284 attachment dishes in mTESR1 medium supplemented with ROCK inhibitor, Y-27632 (10  $\mu$ M;  
285 catalog #1254 Tocris) and basic fibroblast growth factor (FGF-2; 20 ng/mL; catalog #233-FB-010  
286 Tocris) for the first 24 hours to allow for embryoid body (EB) formation. The following day, ROCK  
287 inhibitor was removed, and fresh mTESR1 was added to the cultures. Forty-eight hours after EB  
288 aggregation, cells were switched to MN Differentiation Medium: Advanced DMEM/F-12 (catalog  
289 #12634010 ThermoFisher) & NB Medium (50:50 v/v), 1x N-2 supplement, 1x B27+Insulin, 1x  
290 GlutaMAX (catalog #A1286001 ThermoFisher), 1x pen/strep, and 0.1 mM 2-mercaptoethanol  
291 (catalog #31350010 ThermoFisher). To specify neural patterning, dual SMAD inhibition was used  
292 with small molecules SB431542 (10  $\mu$ M) and LDN193189 (100 nM) from day 0 to day 6 of  
293 differentiation. From day 0 to day 4 the glycogen synthase kinase 3 inhibitor, CHIR99021 (3  $\mu$ M;  
294 catalog #4423 Tocris) was added to increase the population of Olig2 positive MN progenitors.  
295 Beginning on day 2, MN specification was induced with 1  $\mu$ M All-trans Retinoic Acid (at-RA;  
296 catalog #0695 Tocris) and 1  $\mu$ M Smoothed Agonist (SAG; catalog #4366 Tocris; assuming  
297 that's what you used) until day 16. The  $\gamma$ -secretase inhibitor, (2S)-N-[(3,5-Difluorophenyl)acetyl]-  
298 L-alanyl-2-phenylglycine 1,1-dimethylethyl ester (DAPT, catalog #2634 Tocris) was used at 10  
299  $\mu$ M in conjunction with neurotrophic factors BDNF and GDNF (10 ng/mL each) starting on day 8  
300 until day 16 of differentiation, with 50% medium changes every 2 days. Spheroids were then  
301 dissociated with a solution containing 0.25% Trypsin-EDTA and DNase (25  $\mu$ g/mL; catalog  
302 #18047019 ThermoFisher), and plated onto poly-L-ornithine (25  $\mu$ g/mL; catalog #P2533-10MG  
303 Sigma-Aldrich), Fibronectin (10  $\mu$ g/mL; catalog #11051407001 Sigma-Aldrich), and Laminin (10  
304  $\mu$ g/mL)- coated plates in medium supplemented with BDNF and GDNF (10 ng/mL each). See **SI**  
305 **Table 5** for detailed protocol steps and refer to **SI Figure 2** for differentiation protocol outline and  
306 representative images of MN cultures.

307 *Human iPSC-derived astrocyte differentiation and maintenance.* Human NPCs were expanded as  
308 progenitors and then seeded at ~20% confluence onto Matrigel-coated tissue culture plates.  
309 Commercial astrocyte medium (catalog #1801 Sciencell) was used to differentiate NPCs as  
310 previously described [47, 48]. Briefly, starting with ~40% confluent NPC cultures, astrocyte  
311 medium was changed every 3-4 days and cells were passaged at 1:10 ratio when they reached  
312 ~80-90% confluence for the first 28 days. Immature astrocytes generated by this method express  
313 multiple canonical glial markers and were further matured via small molecules or exposure to  
314 FBS/Matrigel into GFAP+ cells [49]. See **SI Figure 3** and **SI Table 6** for detailed protocol and  
315 representative images.

316 *Design of imaging strands for PRISM antibody conjugation.* We designed new DNA imaging  
317 strands and used previously published LNA sequences to generate stable PRISM pairs by varying  
318 their length and altering the GC content of the oligos (**SI Table 7**).

319 *Automated pipeline for antibody staining, imaging, and characterization of cortical cultures.* To  
320 validate PRISM antibodies for automation suitability, we performed IF imaging on two high content  
321 plate confocal microscopes, the PerkinElmer Opera Phenix and the Molecular Devices  
322 ImageXpress. Once antibody signal was confirmed, IF staining of cortical cultures (**SI Figure 10**)  
323 was adapted to 96-well plates and was partially automated using a BRAVO liquid handler (Agilent);  
324 dispensing 100  $\mu$ l of either buffer, antibody, or PRISM reagent per well (See **SI Table 3** for details  
325 on buffer compositions and dilutions). The system was programmed to perform an initial rinse with  
326 Wash Buffer, then each well was aspirated and 100  $\mu$ l of fresh Imaging Buffer with PRISM imaging  
327 strands was added and incubated at room temperature for 10 min. Plates were then rinsed three  
328 times with Imaging Buffer and imaged on a PerkinElmer Opera Phenix at 20X, with the 405 nm

329 laser for Hoechst nuclear stain (IF), 488 nm laser for Actin (IF), and 590 nm and 647 nm lasers for  
330 PRISM antibodies. Exposures were either 300 ms (PRISM antibodies) or 150 ms (ICC controls).  
331 Post-imaging, each well was washed three times with Wash Buffer and incubated for 5 min  
332 between washes to eliminate residual PRISM imaging strand signal. Control imaging was  
333 performed after the third rinse to confirm removal of imaging strands prior to subsequent imaging  
334 strand addition and imaging rounds. These steps were repeated until all PRISM antibodies in the  
335 panel were imaged. Further automation was achieved by incorporating robotics to move the plates  
336 for confocal imaging to the PerkinElmer Opera Phenix high content platform at 60X magnification,  
337 where each well was imaged in a 4x4 tile pattern, covering roughly 10% of the well area. Based  
338 on cell type-specific markers that have been validated in the field (**SI Table 2**), we then built up a  
339 query algorithm to identify each cell subtype we were interested in within the differentiated  
340 cultures. Only cells that were positive for all the required markers were included in the analysis  
341 groups within each sub-type. A detailed breakdown on cellular characterization is shown in **Figure**  
342 **2a**.

343 Data were analyzed using custom CellProfiler (cellprofiler.org) and FIJI (<https://fiji.sc/>) pipelines  
344 for post-processing and image analysis of high-content PRISM data (reference code is available  
345 upon request). Each image from the PRISM assay was aligned in sequential imaging rounds using  
346 the nuclear (Hoechst 33342; 405 nm) and actin (Phalloidin; 488 nm) channels. The aligned signal  
347 from each marker was then overlaid in a composite image that was then analyzed for protein co-  
348 localization within the cells, expression patterns of specific markers in the culture and levels of  
349 protein expression. Only cells that were present in all image sequences of an experiment, based  
350 on the overlays, were fed to the CellProfiler analysis pipeline to characterize the neural cultures.  
351 Sampling data from 12 markers, i.e., 5 probe addition/imaging sequences, allowed us to generate  
352 multi-stain identity of cellular populations that were designated as neurons (cortical or motor),  
353 astrocytes, neural stem cells, etc., building cellular composition profiles of the tested iPSC-derived  
354 cortical and motor neuron cultures.

355

## 356 **DATA AVAILABILITY**

357 The data that support the findings of this study are available from the corresponding author upon  
358 reasonable request.

359 **References**

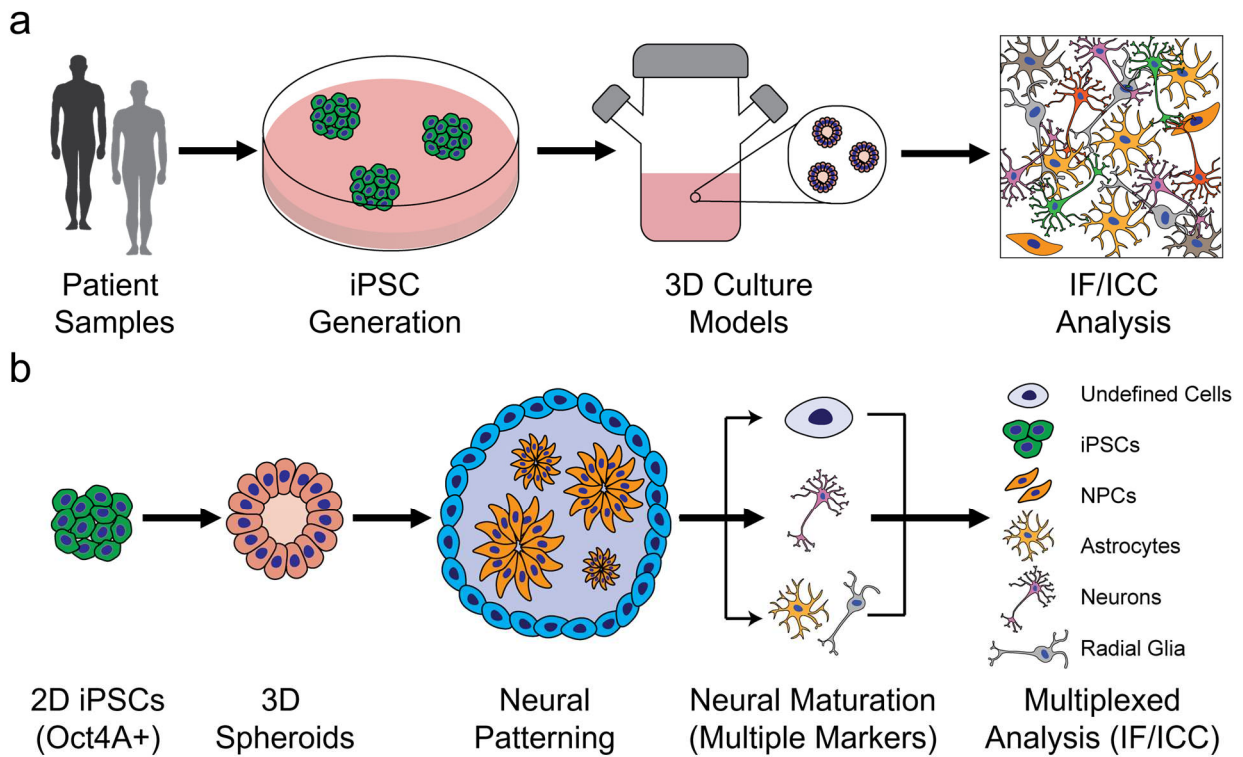
- 360
- 361 1. Andoh-Noda, T., et al., *Modeling Rett Syndrome Using Human Induced Pluripotent Stem*  
362 *Cells*. CNS Neurol Disord Drug Targets, 2016. **15**(5): p. 544-50.
- 363 2. Avior, Y., I. Sagi, and N. Benvenisty, *Pluripotent stem cells in disease modelling and drug*  
364 *discovery*. Nat Rev Mol Cell Biol, 2016. **17**(3): p. 170-82.
- 365 3. Bourgeron, T., *From the genetic architecture to synaptic plasticity in autism spectrum*  
366 *disorder*. Nat Rev Neurosci, 2015. **16**(9): p. 551-63.
- 367 4. Marchetto, M.C., et al., *A model for neural development and treatment of Rett syndrome*  
368 *using human induced pluripotent stem cells*. Cell, 2010. **143**(4): p. 527-39.
- 369 5. Ooi, L., et al., *Induced pluripotent stem cells as tools for disease modelling and drug*  
370 *discovery in Alzheimer's disease*. J Neural Transm (Vienna), 2013. **120**(1): p. 103-11.
- 371 6. Barral, S. and M.A. Kurian, *Utility of Induced Pluripotent Stem Cells for the Study and*  
372 *Treatment of Genetic Diseases: Focus on Childhood Neurological Disorders*. Front Mol  
373 Neurosci, 2016. **9**: p. 78.
- 374 7. Di Giorgio, F.P., et al., *Human embryonic stem cell-derived motor neurons are sensitive to*  
375 *the toxic effect of glial cells carrying an ALS-causing mutation*. Cell Stem Cell, 2008. **3**(6):  
376 p. 637-48.
- 377 8. Di Giorgio, F.P., et al., *Non-cell autonomous effect of glia on motor neurons in an*  
378 *embryonic stem cell-based ALS model*. Nat Neurosci, 2007. **10**(5): p. 608-14.
- 379 9. Lindvall, O. and Z. Kokaia, *Stem cells for the treatment of neurological disorders*. Nature,  
380 2006. **441**(7097): p. 1094-6.
- 381 10. Kulikov, V., et al., *DoGNet: A deep architecture for synapse detection in multiplexed*  
382 *fluorescence images*. PLoS Comput Biol, 2019. **15**(5): p. e1007012.
- 383 11. Guo, S.M., et al., *Multiplexed and high-throughput neuronal fluorescence imaging with*  
384 *diffusible probes*. Nat Commun, 2019. **10**(1): p. 4377.
- 385 12. Micheva, K.D. and S.J. Smith, *Array tomography: a new tool for imaging the molecular*  
386 *architecture and ultrastructure of neural circuits*. Neuron, 2007. **55**(1): p. 25-36.
- 387 13. Micheva, K.D., et al., *Array tomography: high-resolution three-dimensional*  
388 *immunofluorescence*. Cold Spring Harb Protoc, 2010. **2010**(11): p. pdb top89.
- 389 14. Jungmann, R., et al., *Multiplexed 3D cellular super-resolution imaging with DNA-PAINT*  
390 *and Exchange-PAINT*. Nat Methods, 2014. **11**(3): p. 313-8.
- 391 15. Xu, Q., et al., *Design of 240,000 orthogonal 25mer DNA barcode probes*. Proc Natl Acad  
392 Sci U S A, 2009. **106**(7): p. 2289-94.
- 393 16. Buchwalow, I.B., E.A. Minin, and W. Boecker, *A multicolor fluorescence immunostaining*  
394 *technique for simultaneous antigen targeting*. Acta Histochem, 2005. **107**(2): p. 143-8.
- 395 17. Lan, H.Y., et al., *A novel, simple, reliable, and sensitive method for multiple*  
396 *immunoenzyme staining: use of microwave oven heating to block antibody crossreactivity*  
397 *and retrieve antigens*. J Histochem Cytochem, 1995. **43**(1): p. 97-102.
- 398 18. Lewis Carl, S.A., I. Gillete-Ferguson, and D.G. Ferguson, *An indirect immunofluorescence*  
399 *procedure for staining the same cryosection with two mouse monoclonal primary*  
400 *antibodies*. J Histochem Cytochem, 1993. **41**(8): p. 1273-8.
- 401 19. Nieves, D.J., K. Gaus, and M.A.B. Baker, *DNA-Based Super-Resolution Microscopy: DNA-*  
402 *PAINT*. Genes (Basel), 2018. **9**(12).
- 403 20. Schnitzbauer, J., et al., *Super-resolution microscopy with DNA-PAINT*. Nat Protoc, 2017.  
404 **12**(6): p. 1198-1228.
- 405 21. Schueder, F., et al., *Multiplexed 3D super-resolution imaging of whole cells using spinning*  
406 *disk confocal microscopy and DNA-PAINT*. Nat Commun, 2017. **8**(1): p. 2090.
- 407 22. Zanella, F., J.B. Lorens, and W. Link, *High content screening: seeing is believing*. Trends  
408 Biotechnol, 2010. **28**(5): p. 237-45.

- 409 23. Schindelin, J., et al., *Fiji: an open-source platform for biological-image analysis*. Nat  
410 Methods, 2012. **9**(7): p. 676-82.
- 411 24. Carpenter, A.E., et al., *CellProfiler: image analysis software for identifying and quantifying*  
412 *cell phenotypes*. Genome Biol, 2006. **7**(10): p. R100.
- 413 25. Genovese, G., et al., *Increased burden of ultra-rare protein-altering variants among 4,877*  
414 *individuals with schizophrenia*. Nat Neurosci, 2016. **19**(11): p. 1433-1441.
- 415 26. Ripke, S., et al., *Genome-wide association analysis identifies 13 new risk loci for*  
416 *schizophrenia*. Nat Genet, 2013. **45**(10): p. 1150-9.
- 417 27. Gulsuner, S., et al., *Spatial and temporal mapping of de novo mutations in schizophrenia*  
418 *to a fetal prefrontal cortical network*. Cell, 2013. **154**(3): p. 518-29.
- 419 28. van Rheenen, W., et al., *Genome-wide association analyses identify new risk variants and*  
420 *the genetic architecture of amyotrophic lateral sclerosis*. Nat Genet, 2016. **48**(9): p. 1043-  
421 8.
- 422 29. McLaughlin, R.L., et al., *Genetic correlation between amyotrophic lateral sclerosis and*  
423 *schizophrenia*. Nat Commun, 2017. **8**: p. 14774.
- 424 30. Tiziano, F.D., J. Melki, and L.R. Simard, *Solving the puzzle of spinal muscular atrophy:*  
425 *what are the missing pieces?* Am J Med Genet A, 2013. **161A**(11): p. 2836-45.
- 426 31. Yang, C.W., et al., *An Integrative Transcriptomic Analysis for Identifying Novel Target*  
427 *Genes Corresponding to Severity Spectrum in Spinal Muscular Atrophy*. PLoS One, 2016.  
428 **11**(6): p. e0157426.
- 429 32. Lindsay, M.A., *Target discovery*. Nat Rev Drug Discov, 2003. **2**(10): p. 831-8.
- 430 33. Wang, L., et al., *Locked nucleic acid molecular beacons*. J Am Chem Soc, 2005. **127**(45):  
431 p. 15664-5.
- 432 34. Agasti, S.S., et al., *DNA-barcoded labeling probes for highly multiplexed Exchange-PAINT*  
433 *imaging*. Chem Sci, 2017. **8**(4): p. 3080-3091.
- 434 35. Wade, O.K., et al., *124-Color Super-resolution Imaging by Engineering DNA-PAINT*  
435 *Blinking Kinetics*. Nano Lett, 2019. **19**(4): p. 2641-2646.
- 436 36. Betancur, C., *Etiological heterogeneity in autism spectrum disorders: more than 100*  
437 *genetic and genomic disorders and still counting*. Brain Res, 2011. **1380**: p. 42-77.
- 438 37. Walsh, T., et al., *Rare structural variants disrupt multiple genes in neurodevelopmental*  
439 *pathways in schizophrenia*. Science, 2008. **320**(5875): p. 539-43.
- 440 38. International Schizophrenia, C., et al., *Common polygenic variation contributes to risk of*  
441 *schizophrenia and bipolar disorder*. Nature, 2009. **460**(7256): p. 748-52.
- 442 39. Shi, J., et al., *Common variants on chromosome 6p22.1 are associated with schizophrenia*.  
443 Nature, 2009. **460**(7256): p. 753-7.
- 444 40. Fromer, M., et al., *De novo mutations in schizophrenia implicate synaptic networks*. Nature,  
445 2014. **506**(7487): p. 179-84.
- 446 41. Schizophrenia Working Group of the Psychiatric Genomics, C., *Biological insights from*  
447 *108 schizophrenia-associated genetic loci*. Nature, 2014. **511**(7510): p. 421-7.
- 448 42. Dale, J.M., et al., *The spinal muscular atrophy mouse model, SMADelta7, displays altered*  
449 *axonal transport without global neurofilament alterations*. Acta Neuropathol, 2011. **122**(3):  
450 p. 331-41.
- 451 43. Rigamonti, A., et al., *Large-Scale Production of Mature Neurons from Human Pluripotent*  
452 *Stem Cells in a Three-Dimensional Suspension Culture System*. Stem Cell Reports, 2016.  
453 **6**(6): p. 993-1008.
- 454 44. Lancaster, M.A. and J.A. Knoblich, *Generation of cerebral organoids from human*  
455 *pluripotent stem cells*. Nat Protoc, 2014. **9**(10): p. 2329-40.
- 456 45. Maury, Y., et al., *Combinatorial analysis of developmental cues efficiently converts human*  
457 *pluripotent stem cells into multiple neuronal subtypes*. Nat Biotechnol, 2015. **33**(1): p. 89-  
458 96.

- 459 46. Du, Z.W., et al., *Generation and expansion of highly pure motor neuron progenitors from*  
460 *human pluripotent stem cells*. Nat Commun, 2015. **6**: p. 6626.
- 461 47. Pasca, A.M., et al., *Functional cortical neurons and astrocytes from human pluripotent*  
462 *stem cells in 3D culture*. Nat Methods, 2015. **12**(7): p. 671-8.
- 463 48. Tomov, M.L., et al., *Distinct and Shared Determinants of Cardiomyocyte Contractility in*  
464 *Multi-Lineage Competent Ethnically Diverse Human iPSCs*. Sci Rep, 2016. **6**: p. 37637.
- 465 49. So, P.T., et al., *Two-photon excitation fluorescence microscopy*. Annu Rev Biomed Eng,  
466 2000. **2**: p. 399-429.

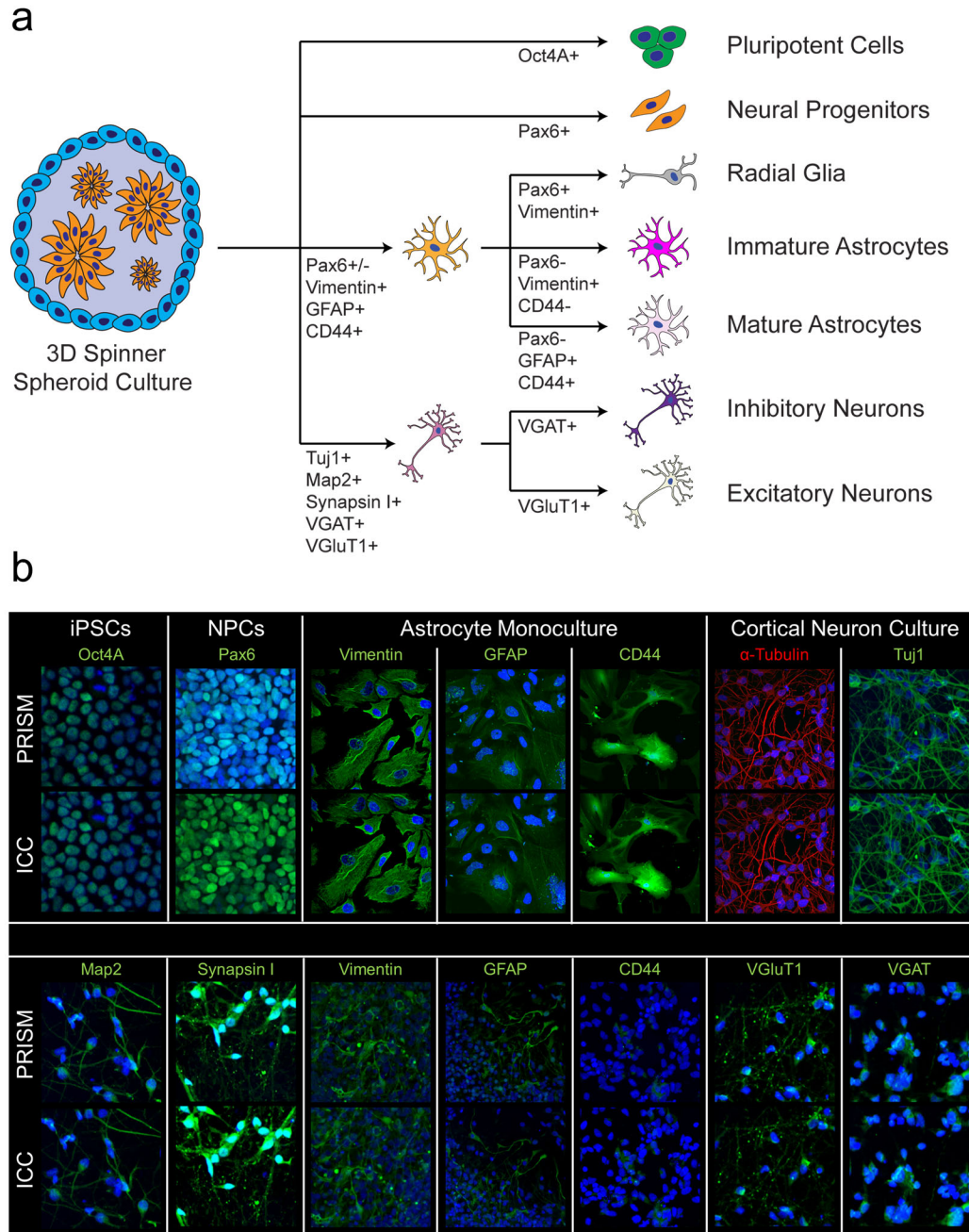
467

468



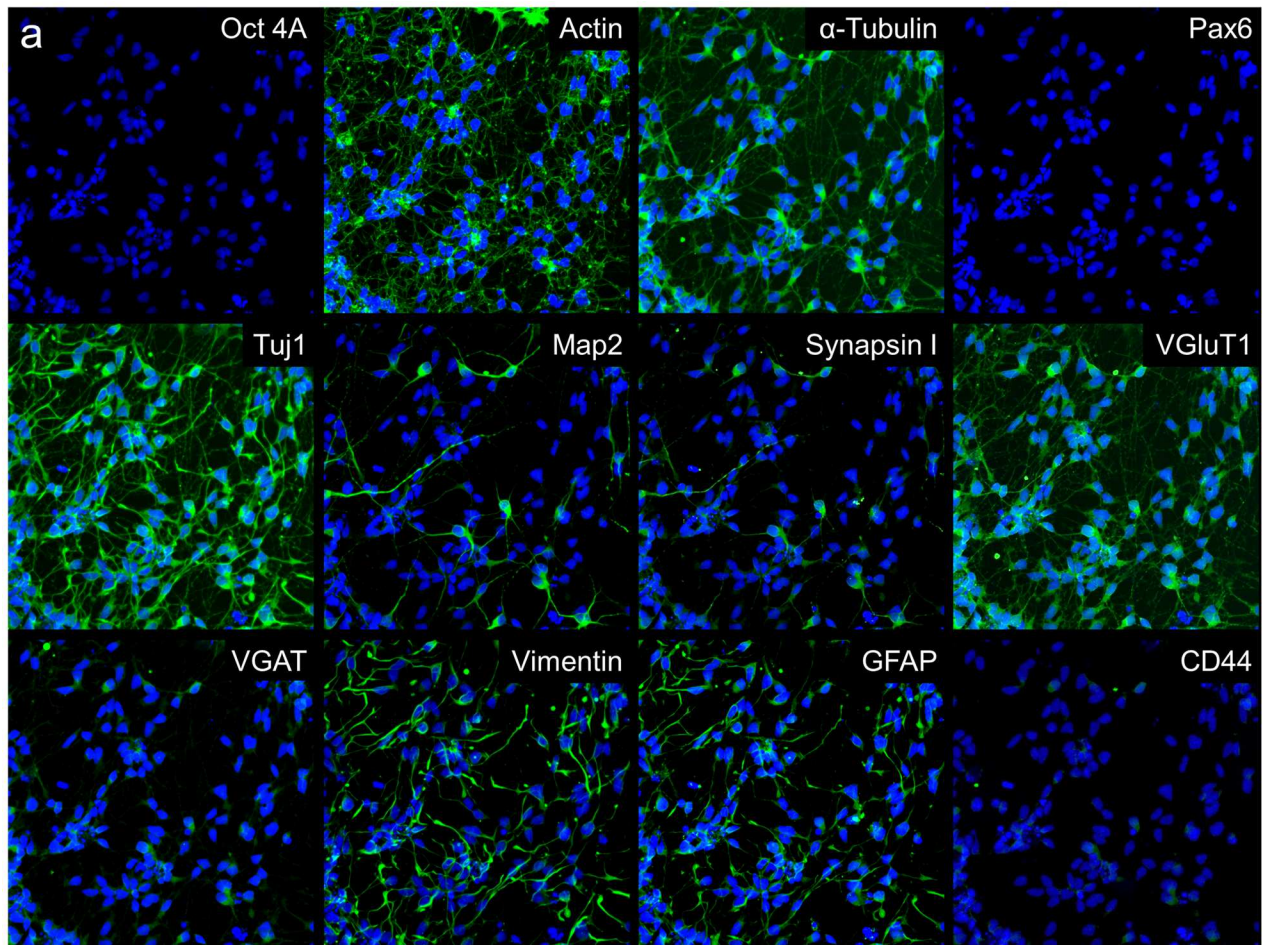
470

471 **Figure 1: Generating stem cell derived disease models and complex neuronal cultures**  
 472 **based on patient iPSCs requires careful and extensive validation. (a)** Process flow to  
 473 generate disease-specific stem cell lines from patients to model *in vitro* complex  
 474 neurodevelopmental and neurodegenerative diseases using 3D spheroid cultures of cortical and  
 475 motor neurons. **(b)** Stem cell-derived 3D neural cultures used to generate high-content data for  
 476 culture and disease modeling. Cells are subsequently analyzed to generate specific culture  
 477 breakdowns using PRISM for in-depth characterization of neural cultures via multiplexed staining.

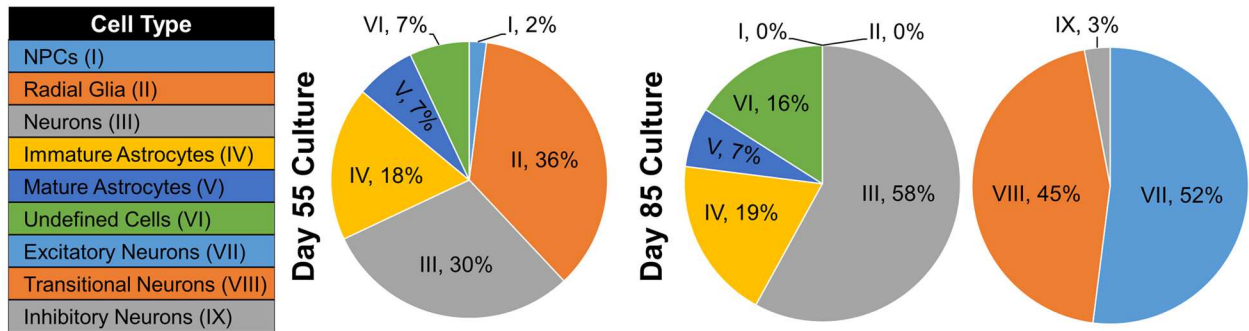


478

479 **Figure 2: Breakdown of cell populations present in iPSC-derived neural cultures and**  
 480 **validation staining of marker panel targets used in the in-depth characterization.** A  
 481 schematic **(a)** of the different cell types in a typical cortical culture that can be tracked via PRISM.  
 482 The flow chart illustrates a representative readout of the breakdown of cell populations in cortical  
 483 cultures. **(b)** ICC versus PRISM images of the markers used to characterize neural cultures. The  
 484 Oct4A marker was imaged in the undifferentiated pluripotent state cell culture (iPCS), and the  
 485 PAX6 marker was imaged in day 14 neural progenitor state cell culture (NPCs) for validation  
 486 purposes.



**b**

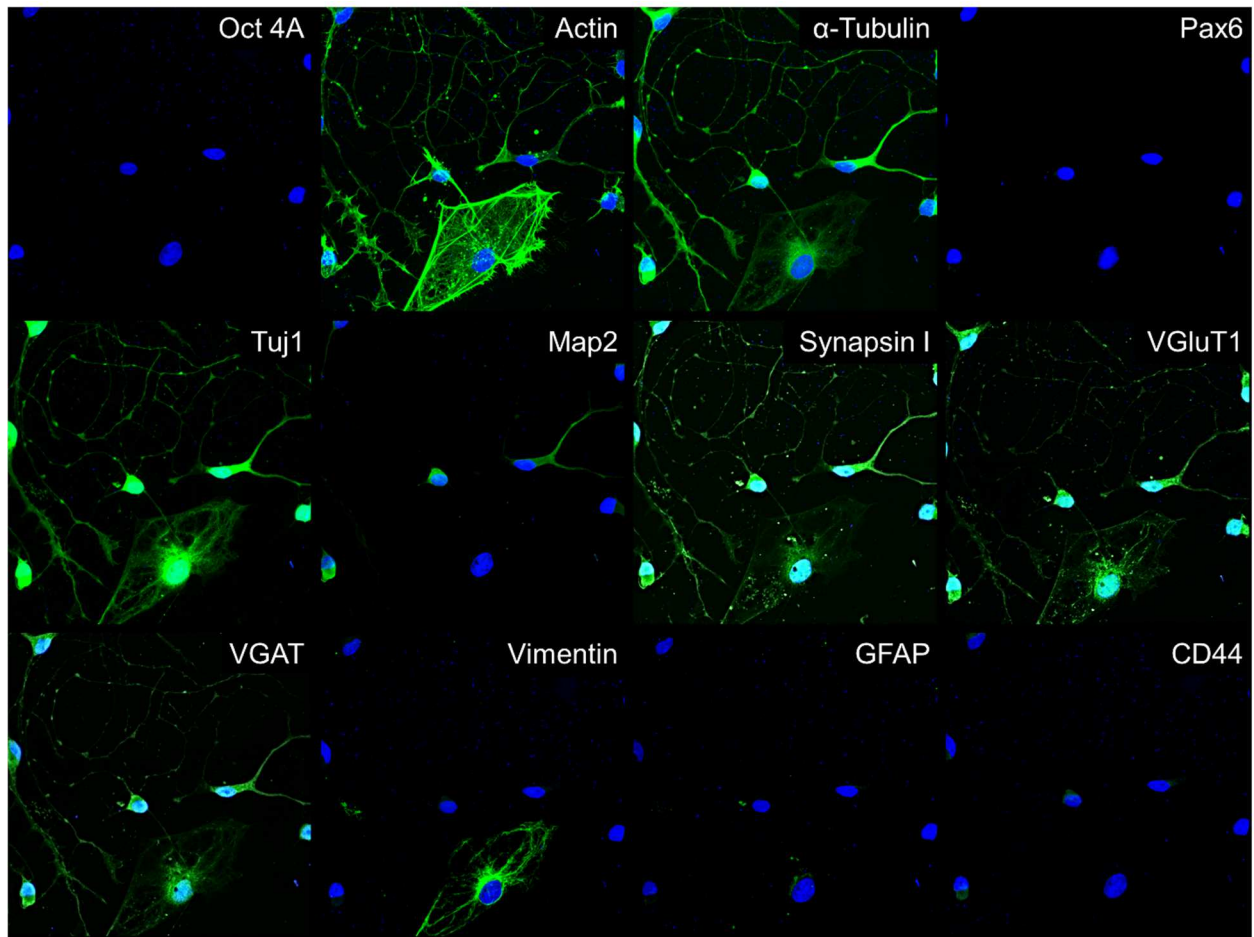


487

488 **Figure 3: High-content analysis of dissociated cultures from hiPSC-derived cortical**  
 489 **neurons. (a)** Representative images from the same area of a 71 days old BJ-SiPs-derived cortical  
 490 neuron culture, stained with the optimized 12-marker PRISM antibody panel, 14 days post-  
 491 dissociation into 2D cultures. **(b)** CellProfiler quantification of cell types at 55 and 85 days in culture  
 492 respectively.

493

494



495 **Figure 4: High-content IF/ICC analysis of dissociated cultures from hiPSC-derived motor**  
496 **neuron culture.** Representative images from the same area of a 1016A-derived motor neuron  
497 culture, stained with the optimized 12-marker PRISM antibody panel after being grown for 21 days  
498 as a 3D spheroid, then dissociated into 2D and maintained for 14 days.

# Figures

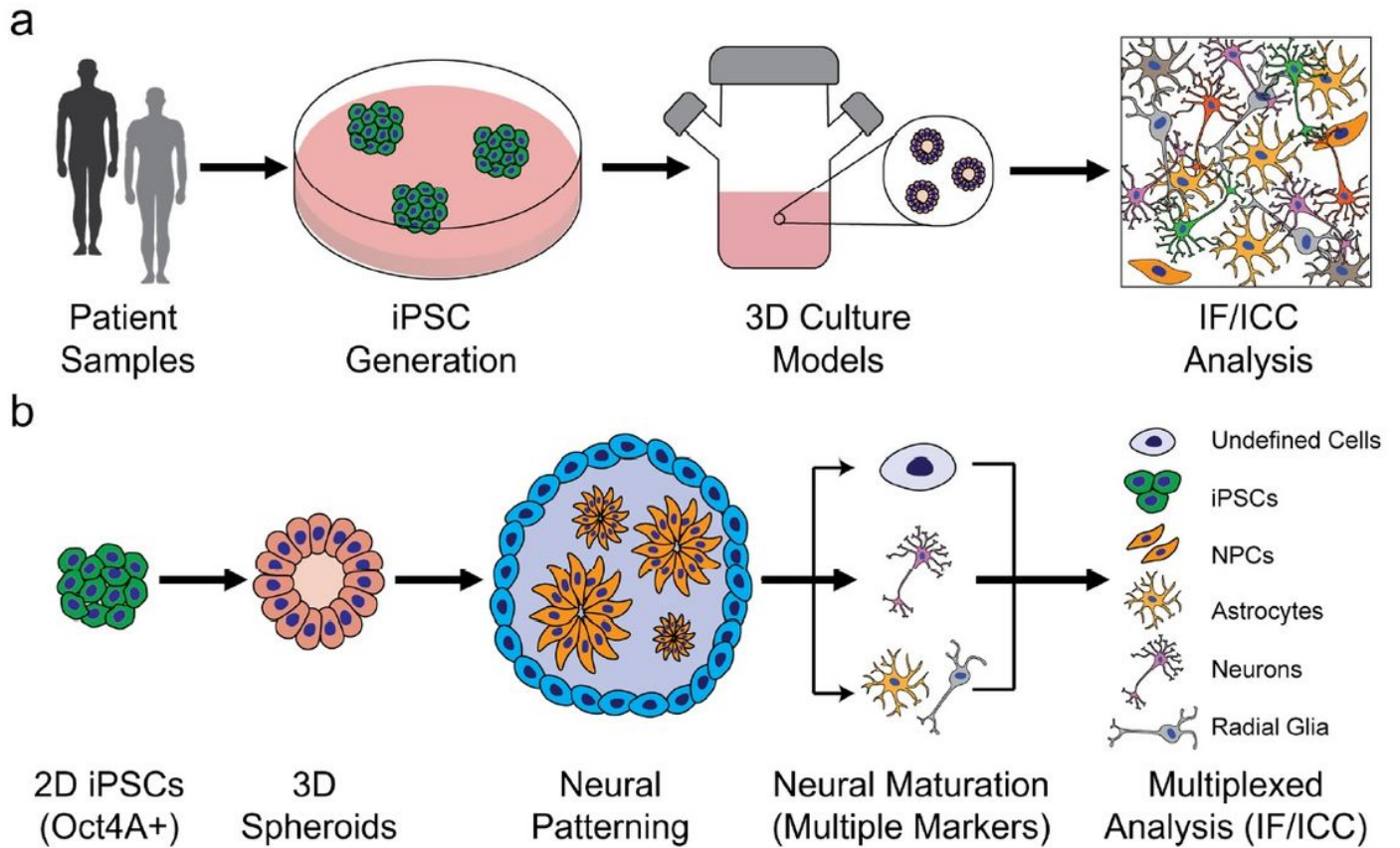


**Figure 1**

Generating stem cell derived disease models and complex neuronal cultures based on patient iPSCs requires careful and extensive validation. (a) Process flow to generate disease-specific stem cell lines from patients to model in vitro complex neurodevelopmental and neurodegenerative diseases using 3D spheroid cultures of cortical and motor neurons. (b) Stem cell-derived 3D neural cultures used to generate high-content data for culture and disease modeling. Cells are subsequently analyzed to generate specific culture breakdowns using PRISM for in-depth characterization of neural cultures via multiplexed staining.

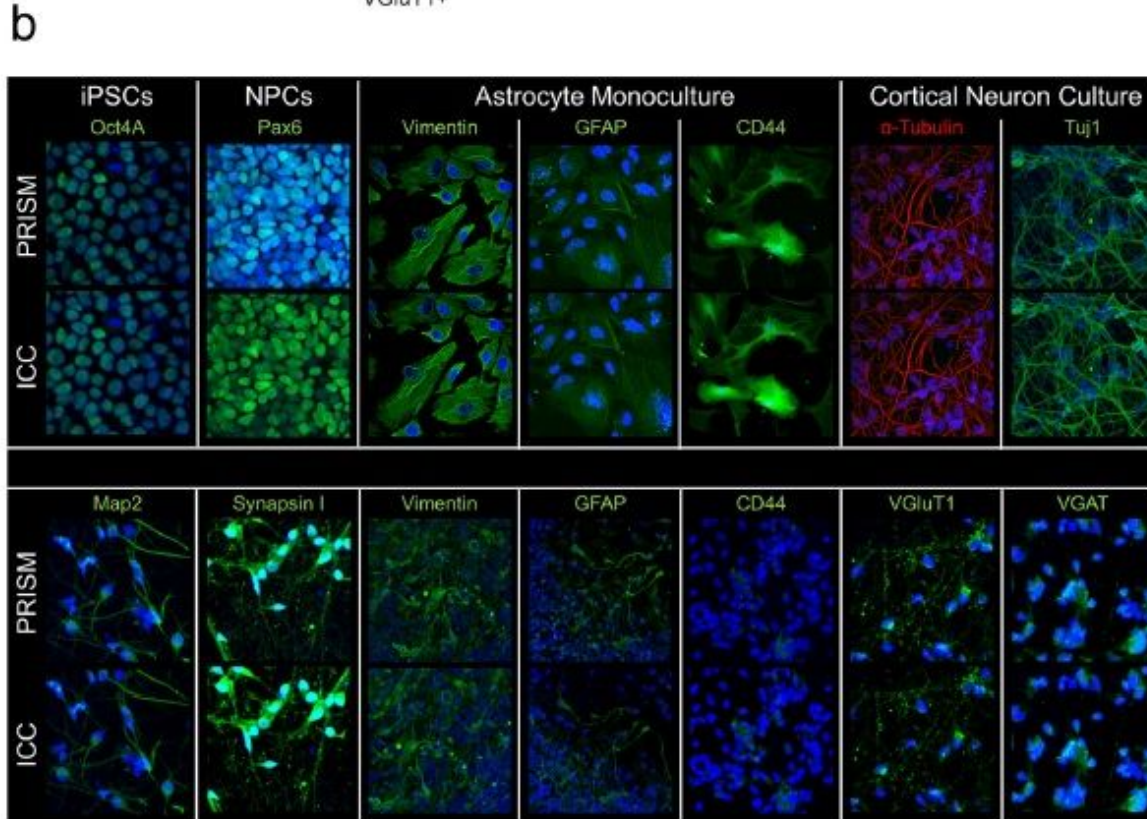
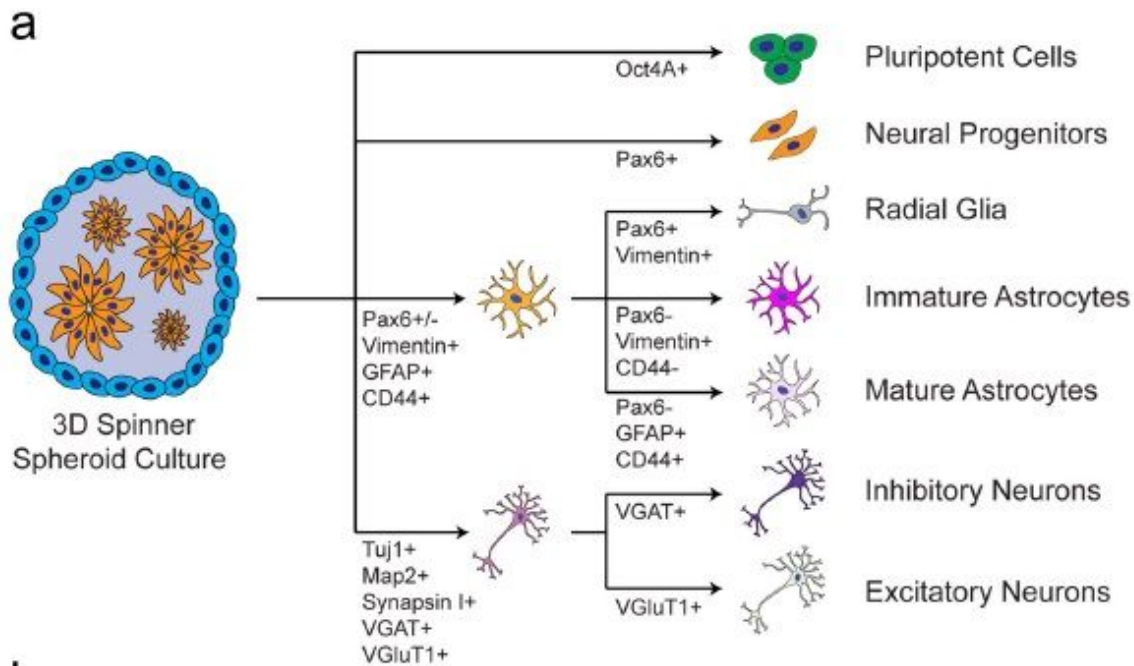


**Figure 2**

Breakdown of cell populations present in iPSC-derived neural cultures and validation staining of marker panel targets used in the in-depth characterization. A schematic (a) of the different cell types in a typical cortical culture that can be tracked via PRISM. The flow chart illustrates a representative readout of the breakdown of cell populations in cortical cultures. (b) ICC versus PRISM images of the markers used to characterize neural cultures. The Oct4A marker was imaged in the undifferentiated pluripotent state cell

culture (iPCS), and the PAX6 marker was imaged in day 14 neural progenitor state cell culture (NPCs) for validation purposes.

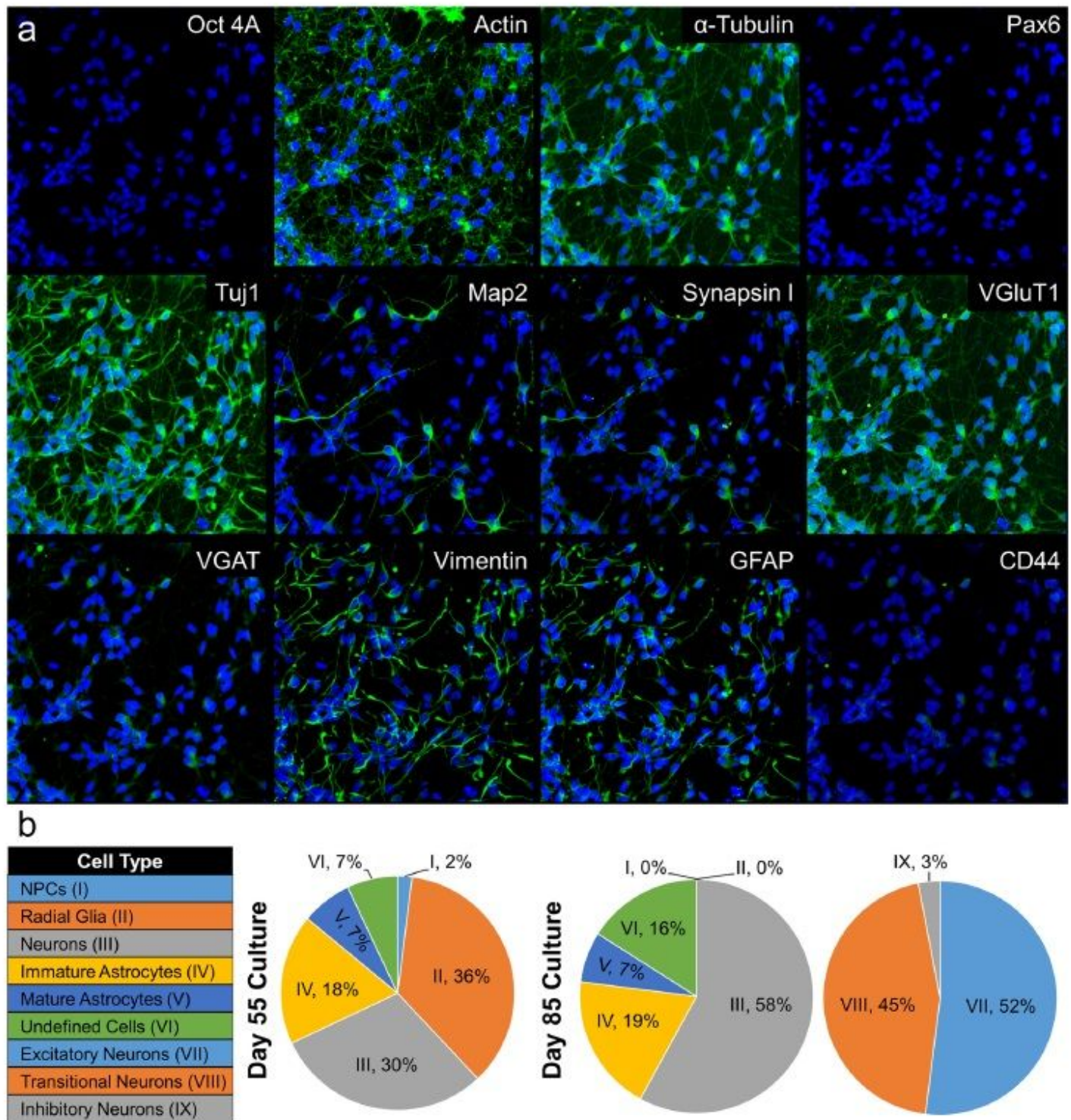


**Figure 3**

High-content analysis of dissociated cultures from hiPSC-derived cortical neurons. (a) Representative images from the same area of a 71 days old BJ-SiPs-derived cortical 490 neuron culture, stained with the

optimized 12-marker PRISM antibody panel, 14 days post dissociation into 2D cultures. (b) CellProfiler quantification of cell types at 55 and 85 days in culture respectively.

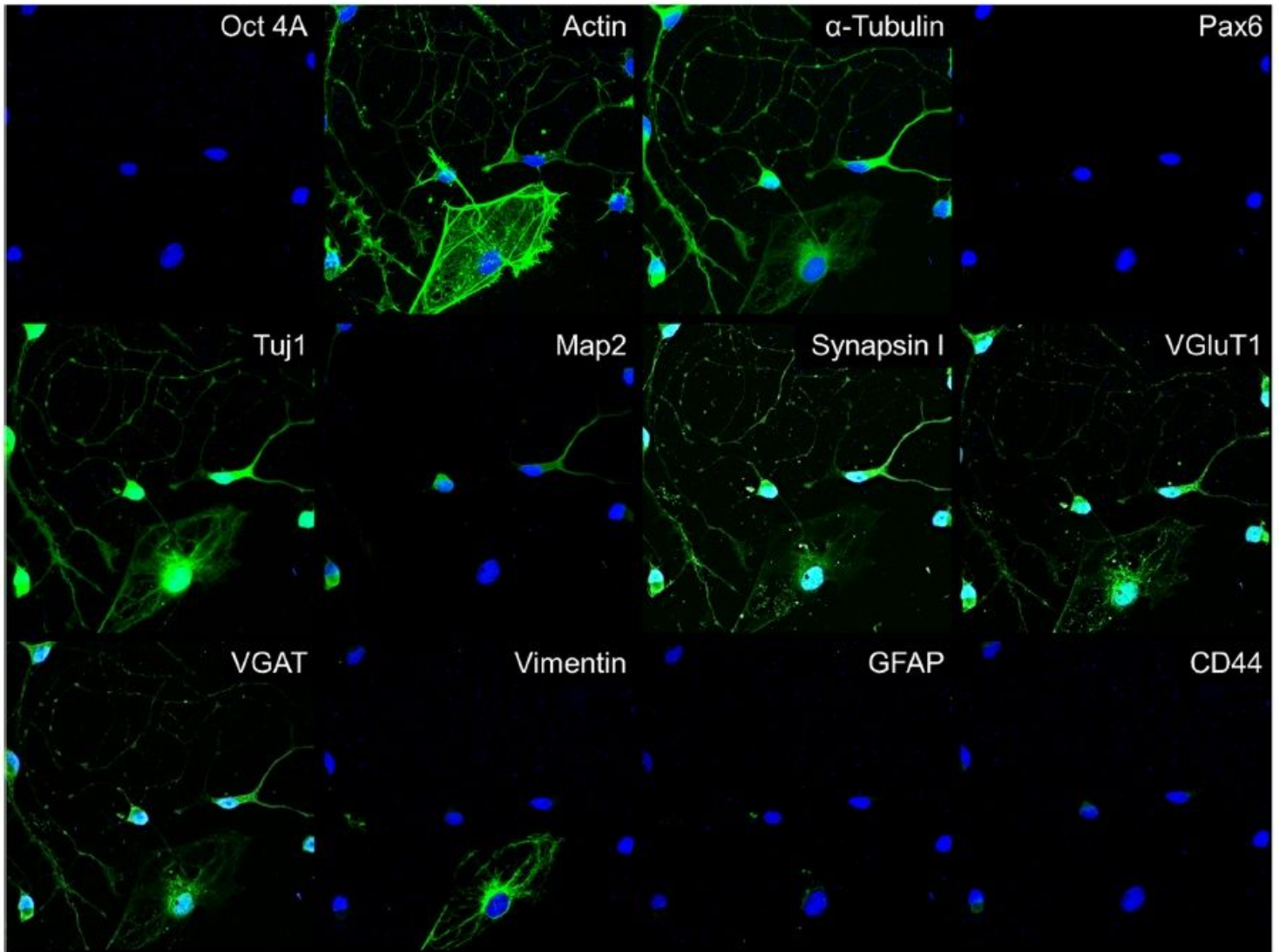


**Figure 4**

High-content IF/ICC analysis of dissociated cultures from hiPSC-derived motor neuron culture. Representative images from the same area of a 1016A-derived motor neuron culture, stained with the optimized 12-marker PRISM antibody panel after being grown for 21 days as a 3D spheroid, then dissociated into 2D and maintained for 14 days.

## Supplementary Files

This is a list of supplementary files associated with this preprint. Click to download.

- [ManuscriptMTomovSINatCommBio.pdf](#)